ELECTRONIC SUPPORTING INFORMATION

Facile meltPEGylation of Flame-made Luminescent Tb^{3+}-doped Yttrium Oxide Particles: Hemocompatibility, Cellular Uptake and Comparison to Silica

*Kerda Keevend, Guido Panzarasa, Fabian H. L. Starsich, Martin Zeltner, Anastasia Spyrogianni, Elena Tsolaki, Giuseppino Fortunato, Sotiris E. Pratsinis, Sergio Bertazzo, Inge K. Herrmann**

**inge.herrmann@empa.ch*

Experimental

Nanoparticle synthesis. Yttrium oxide nanoparticles were synthesized by flame pyrolysis according to the procedure described by Sotiriou et al.[38] Briefly, yttrium nitrate (Aldrich, 99.9%) was dissolved in a 1/1 (vol %) mixture of 2-ethylhexanoic acid and ethanol at a molarity of 0.5 M. Terbium was added as a dopant at a concentration of 4 at% using $Tb(NO_3)_3$ (Aldrich, 99.9%) in the above solution. This precursor solution was fed into the spray nozzle at a volumetric flow rate of 5 mL min^{-1} and dispersed by 5 L min^{-1} of O_2. Silica nanoparticles were produced using hexamethyldisiloxane (HMDSO) in ethanol at 0.8 M silicon concentration. The precursor solutions were fed at 5 mL/min to the flame spray nozzle, dispersed by 5 L min^{-1} of O_2 with approximately 1.5 bar pressure drop at the nozzle tip and ignited by a premixed 1.5 L min^{-1} CH_4 and 3.2 L min^{-1} O_2 supporting flame.[1] Particles were collected on a filter downstream of the flame and subsequently subjected to physicochemical characterization.

Particle characteriazation. TEM images of nanoparticles were obtained by suspending particles in ethanol and dropping 10 μL of the resulting suspension on a Formvar copper mesh (Electron Microscopy Science, Lucerna-Chem AG, Lucerne, Switzerland). After drying, the grid was imaged in a JEOL 2000FX transmission electron microscope (TEM). X-ray diffraction patterns (XRD) were recorded with a Bruker D8 advance diffractometer (40 kV, 40 mA, CuKα radiation). Specific surface area was determined by nitrogen adsorption at 77 K using a five-point BET isotherm (TriStar II Plus, Micromeritics) after degassing the nanoparticle samples for 2 h at 150 degC in N_2. Fluorescence spectroscopy was performed using a Quantaurus-QY C11347-11, Hamamatsu Spectrometer, using an excitation wavelength of 254 nm.

PEGylation. Poly(ethylene glycol) monomethyl ether (avg. M_n ~ 350 g mol^{-1}, 1900 g mol^{-1} and 5000 g mol^{-1}), ethanol (anhydrous) and dichloromethane were purchased from Sigma-Aldrich and used as received.

For meltPEGylation (meltPEG), 0.05 g of particles were grand in a mortar together with 1.5 g of poly(ethylene glycol) monomethyl ether. Then, 30 mL of ethanol was added, the suspension was transferred in a double-necked 100 mL round-bottomed flask, sonicated for 30 min and eventually the ethanol was evaporated under vacuum. The solid was heated to 200 degC under inert atmosphere (argon) for 4 h. Then, the flask was allowed to cool to room temperature and 30 mL of dichloromethane was added under sonication. The suspension was sonicated for 30 min and left for 10 min without stirring. The supernatant was centrifuged at 7800 rpm for 30 min. The sediment was re-dispersed two more times

in dichloromethane, then three times in ethanol and eventually three times in water using the same centrifugation and re-dispersion procedure. The concentration of the final suspension in water was determined gravimetrically. In this way, the samples meltPEG350, meltPEG1900 and meltPEG5000 are obtained.

For physisorption (physPEG), 0.05 g of particles were grand together with 1.5 g of poly(ethylene glycol) monomethyl ether. Then, 30 mL of dichloromethane was added, the suspension was transferred in a 50 mL-vial, sonicated for 1.5 h and left under stirring overnight. The suspension was left for 10 min without stirring and the supernatant was centrifuged at 7800 rpm for 30 min. The sediment was re-dispersed two more times in dichloromethane, then three times in ethanol and eventually three times in water using the aforementioned centrifugation and re-dispersion procedure. The concentration of the final suspension in water was determined gravimetrically. In this way, the samples physPEG350, physPEG1900 and physPEG5000 are obtained.

For PEG-silane functionalization, the modified method by Lucky *et al.*[2] was used. Briefly, 0.05 g of nanoparticles were dispersed in ethanol with the aid of ultrasonication. Meanwhile, 0.05 g of mPEG-silane (avg. Mn ~ 350 g mol^{-1}, and 5000 g mol^{-1}, Nanocs Inc., New York, USA) was dissolved in 50 ml of water and nanoparticles were added to the solution. The mixture was stirring for 30 min at room temperature. At the end of the stirring, 1.875 ml of ammonia (28 wt%, Sigma Aldrich) was added dropwise to the mixture and was allowed to mix for 3 hours. Nanoparticles were collected by centrifugation at 10000 g for 15 min, washed three times with ethanol and dried in the oven at 70 degC overnight.

CHN Analysis. Carbon, hydrogen and nitrogen (CHN) content of the samples were measured by vario MICRO cube (Elementar). The micro analyzer was calibrated with sulfanilamide. 2 mg of sample were oxidized/pyrolized over a period of 70 seconds (standard program: 2mg70s). Most of the samples were measured in duplicate.

FTIR. Infrared absorption spectra were measured using Varian 640-IR spectrometer equipped with diamond attenuated total reflectance (ATR) optics.

Particle sedimentation. The stability of Tb^{3+}-doped PEGylated nanocrystals (physisorption vs. meltPEGylation, M_n ~ 350 g mol^{-1}) was assessed using a Cary Varian 500 UV/VIS spectrometer. Sedimentation kinetics was measured in disposable polystyrene macro cuvettes monitoring the absorption only on the top 3-mm suspension layer by partially covering the cuvette. The total volume used in the measurements was 2.1 ml. The linear concentration range was determined by measuring a calibration curve at 350 nm (concentrations: 0, 25, 50, 100 µg/mL). Kinetic absorbance measurements were carried out for 24 hours with particle concentration 100 µg/mL. The measurements were carried out at 23 degC in water. The measurement cuvette was sealed with Parafilm to avoid evaporation from the cuvette.

DLS. Hydrodynamic size measurements were performed using a dynamic light scattering (DLS) ZetaSizer90 instrument from Malvern.

XPS. Surface elemental compositions of the powders were characterized by XPS measurements, performed on a PHI 5000 VersaProbe II instrument (USA) with a monochromatic AlKα X-ray source. Energy resolution of the spectrometer was set to 0.8 eV/step at a pass-energy of 187.85 eV for survey scans and 0.100 eV/step and 23.5 eV pass-energy for high resolution region scans, respectively. Carbon 1s at 284.5 eV was used as a calibration reference to correct for charge effects. Elemental compositions were determined using instrument dependent atom sensitivity factors. The photoelectron-transitions C1s, O1s, Y3d and Si2p were selected to determine the elemental concentrations and the chemical shifts within the region scans. Data analysis was performed by use of CasaXP software (Casa Software Ltd, United Kingdom).

Hemolysis. After obtaining written informed consent (ethical approval, EKSG 12/111), whole blood from healthy volunteers was collected in tubes containing 0.109 M sodium citrate. Tubes were centrifuged at 800 x g. Blood plasma was collected for coagulation measurements. The hemolysis assay was carried out following previously described procedures. Briefly, red blood cells were washed in PBS and the hemoglobin concentration was adjusted to ~30 mg/mL. Blood was incubated with nanoparticle suspensions at the ratio of 1:10 (final nanoparticle concentration 100 μg/mL). Triton X (1%) served as positive and PBS as negative control. After incubation for 3 h at 37 degC the samples were centrifuged at 6000 x g for 10 min. Then, 100 μL of each supernatant was transferred to a well on a 96-well flat-bottom plate. Absorption at 570 nm (hemoglobin) was measured using a Mithras2 LB 943 plate reader.

Coagulation. Plasma coagulation was measured immediately after blood collection. Nanoparticle suspensions were added to fresh citrated plasma at a dilution of 1:10 to reach a final particle concentration of 100 μg/mL. Aerosil200 (Evonik, 0.25 mg per mL) served as positive control, plasma containing 10% H_2O (vehicle) served as negative control. Plasma samples were incubated for 20 minutes at 37 degC and centrifuged at 6000x g. Supernatants (100 μL) were then transferred to a 96well plate and 65 μL of 50 mM $CaCl_2$ solution was added immediately before starting the kinetic measurement. Absorbance at 405 nm (indicative of fibrin polymerization) was observed over time using a Mithras2 LB 943 plate reader.

Uptake study using flow cytometry. For nanoparticle uptake measurements, functionalized nanoparticles (50 μg/mL) were incubated with human monocyte cells (THP-1 cell line, ECACC 88081201) at a concentration of 10^6 cells/mL for 30 minutes, 2 hours and 6 hours, respectively. Untreated and water treated cells served as negative controls. Cells were assessed with Beckmann & Coulter Gallios TM Flow Cytometer (10 000 events gated in forward/side scatter or 2 min maximum acquisition time) in combination with Kaluza Analysis software. The shift of cell population after nanoparticle incubation was recorded with forward and side scatter.

Preparation of cellular specimens for uptake studies. Human monocyte cells (THP-1 cell line) were cultured in Roswell Park Memorial Institute Medium (RPMI-1640) containing 10% fetal bovine serum (FBS) at 37 degC in a humidified 5% CO_2 atmosphere. Cells were sub-cultured every seventh day. For experiments, cells were seeded at a density of 10^6 cells/mL in RPMI-1640 containing 10% FBS. Next, cells were incubated with non-functionalized, meltPEG350 and physPEG350 Y_2O_3:Tb^{3+} nanoparticles (50 μg for 100 000 cells) for 2 hours. Cells were centrifuged at 500 xg for 5 minutes, washed gently with pre-warmed PBS, and fixed with 4% methanol-free paraformaldehyde (PFA) overnight at 4 degC in the fridge. Pellets were then washed with ddH_2O (3x) and cacodylate buffer (0.1M) (3x) and stained with 2% osmium tetroxide and 1.5% potassium ferricyanide for 1 hour. Pellets were washed with ddH_2O and then gradually dehydrated using an ethanol gradient (20%, 40%, 50%, 60 %, 70%, 80%, 90%, 95%, 100% (3x)) and embedded in epoxy resin (EPON 812), according to procedures described in the manufacturer's protocol. Resin blocks were cured in the oven at 60 degC for 48 hours, trimmed with a razor blade and then sectioned in 100nm sections using an ultramicrotome. The thin sections were imaged in a JEOL 2000FX transmission electron microscope.

Statistical analysis. Statistical analysis was performed in SPSS (IBM, Version 23). After testing for distribution, a non-parametric Mann-Whitney-U test was applied. In order to assess correlation between PEGylation density (independent variable) and hemolysis (dependent variable), Spearman's rho was calculated ($N \geq 9$).

Particle characterization

The specific surface area measured by N_2 adsorption (BET method) was 230 m^2 g^{-1} for silica and 71 m^2 g^{-1} for Tb^{3+}-doped yttria nanoparticles. The corresponding average primary particle sizes (d_{BET}) were 10 nm for SiO_2 and 16 nm for Y_2O_3:Tb^{3+}, in line with values reported in literature obtained under comparable process conditions.[3, 4]

Y_2O_3:Tb^{3+} nanoparticles are monoclinic and highly crystalline, while silica is amorphous, which is in good agreement with the literature.[3, 5] The carbon content of as-prepared nanoparticles prior to surface modification determined by elemental analysis (CHN analysis) was <0.1 wt%.

	PEG content (wt% C)		
	Phys	*Melt*	*Silane*
Y_2O_3PEG350	3.32	5	1.32
Y_2O_3PEG1900	3.07	4.06	-
Y_2O_3PEG5000	2.78	3.5	1.83
SiO_2PEG350	0.32	10.52	1.56
SiO_2PEG1900	1.06	4.73	-
SiO_2PEG5000	1.99	7.95	2.25

Hydrodynamic sizes were measured by the means of dynamic light scattering (DLS) (**Figure 1**c). The polydispersity indices (PDI) (see **Figure S3a**) were generally smaller for meltPEGylated particles compared to the values observed for physisorbed PEG particles. In cell culture medium, meltPEGylated Y_2O_3:Tb^{3+} nanoparticles remained much smaller compared to physisorbed PEG nanoparticles (**Figure S3** for raw data). While hydrodynamic sizes of PEGylated silica nanoparticles were significantly larger in cell culture medium compared to water, non-functionalized silica nanoparticles remained remarkably small in serum-containing medium. This is in agreement with previous reports showing high stability of non-functionalized silica at similar concentrations in cell culture medium over time.[6]

Nanoparticle sedimentation kinetics was studied by means of UV-Vis spectroscopy. Sedimentation was monitored in a 3 mm deep suspension layer over 8 hrs by UV-Vis spectroscopy (**Figure 1d**). Non-functionalized Y_2O_3:Tb^{3+} nanoparticles show fast sedimentation within the first 30 minutes, similar to those functionalized by the physisorption route.

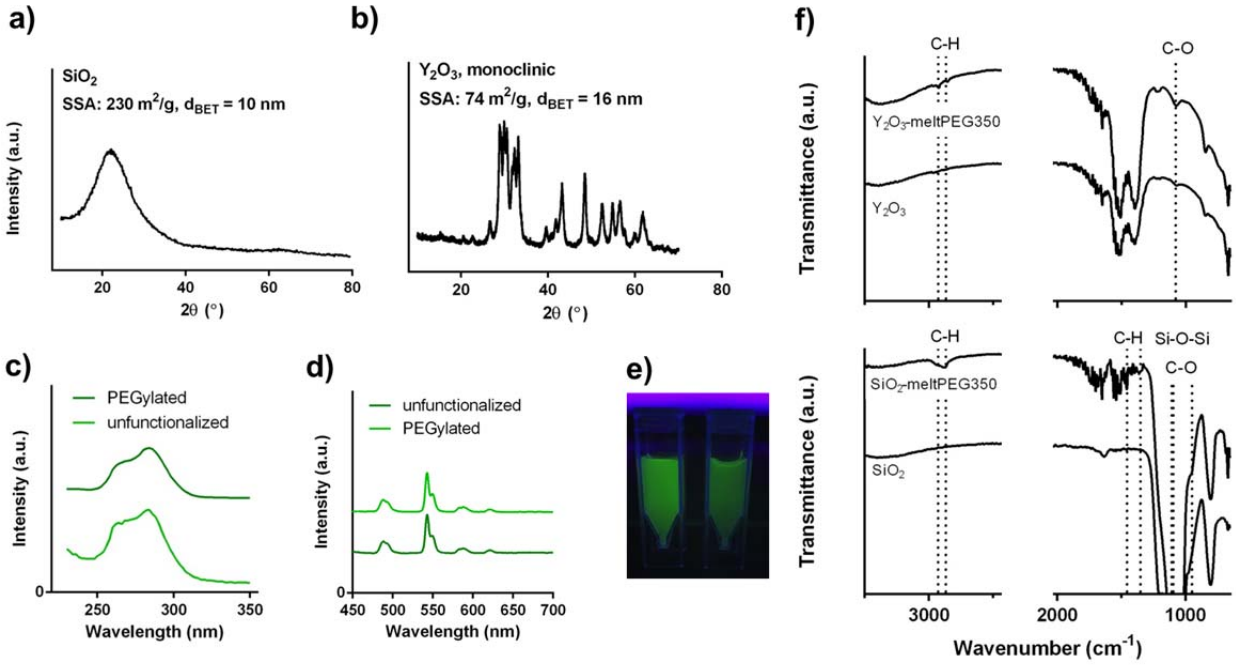

Figure S1*: X-ray diffraction patterns of silica (a) and Tb^{3+}-doped yttria nanoparticles (b). Excitation (c) and emission (d) spectra for terbium-doped yttria nanoparticles before and after PEGylation. Photograph of Tb^{3+}-doped yttria nanoparticles under UV excitation (254 nm) (e). FTIR spectra of meltPEGylated silica and yttria nanoparticles (f).*

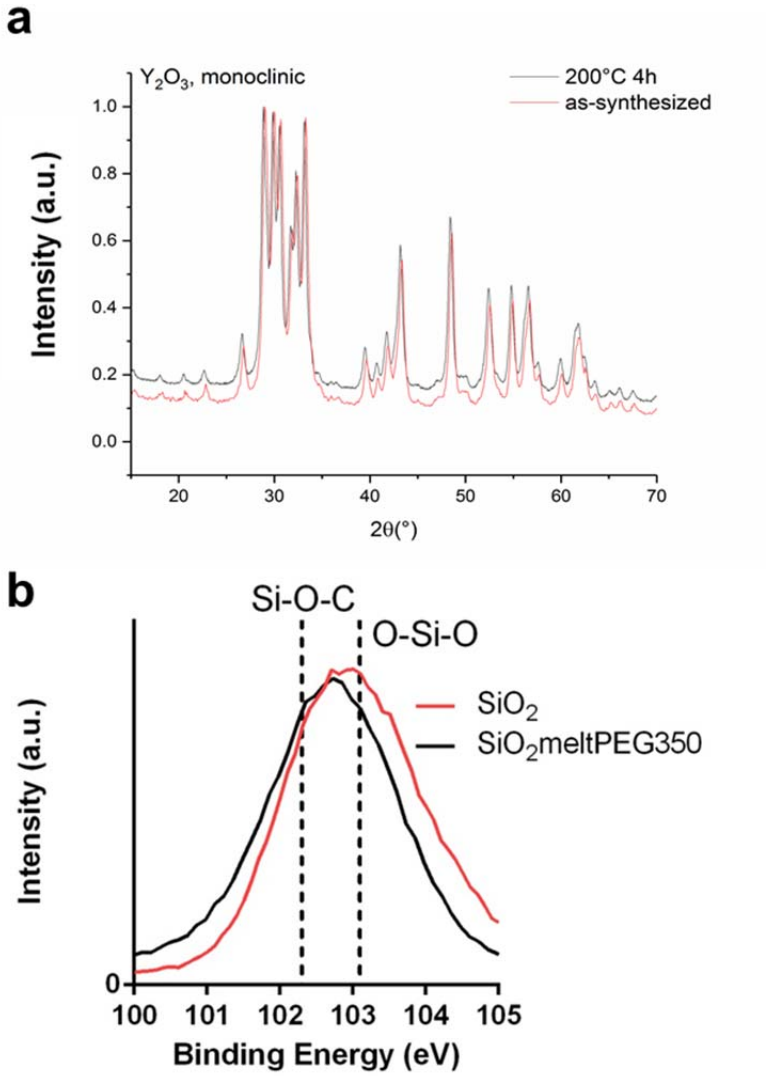

Figure S2: *XRD pattern before and after temperature treatment (4 hours at 200°C, melt PEGylation) shows no apparent phase change (a).XPS analysis (Si2p transition) of non-functionalized and meltPEGylated silica. While a small chemical shift towards the Si-O-C can be seen for the meltPEG nanoparticles, the Si-O-C peak and O-Si-O peak show significant overlap in agreement with previous reports (b).*[7]

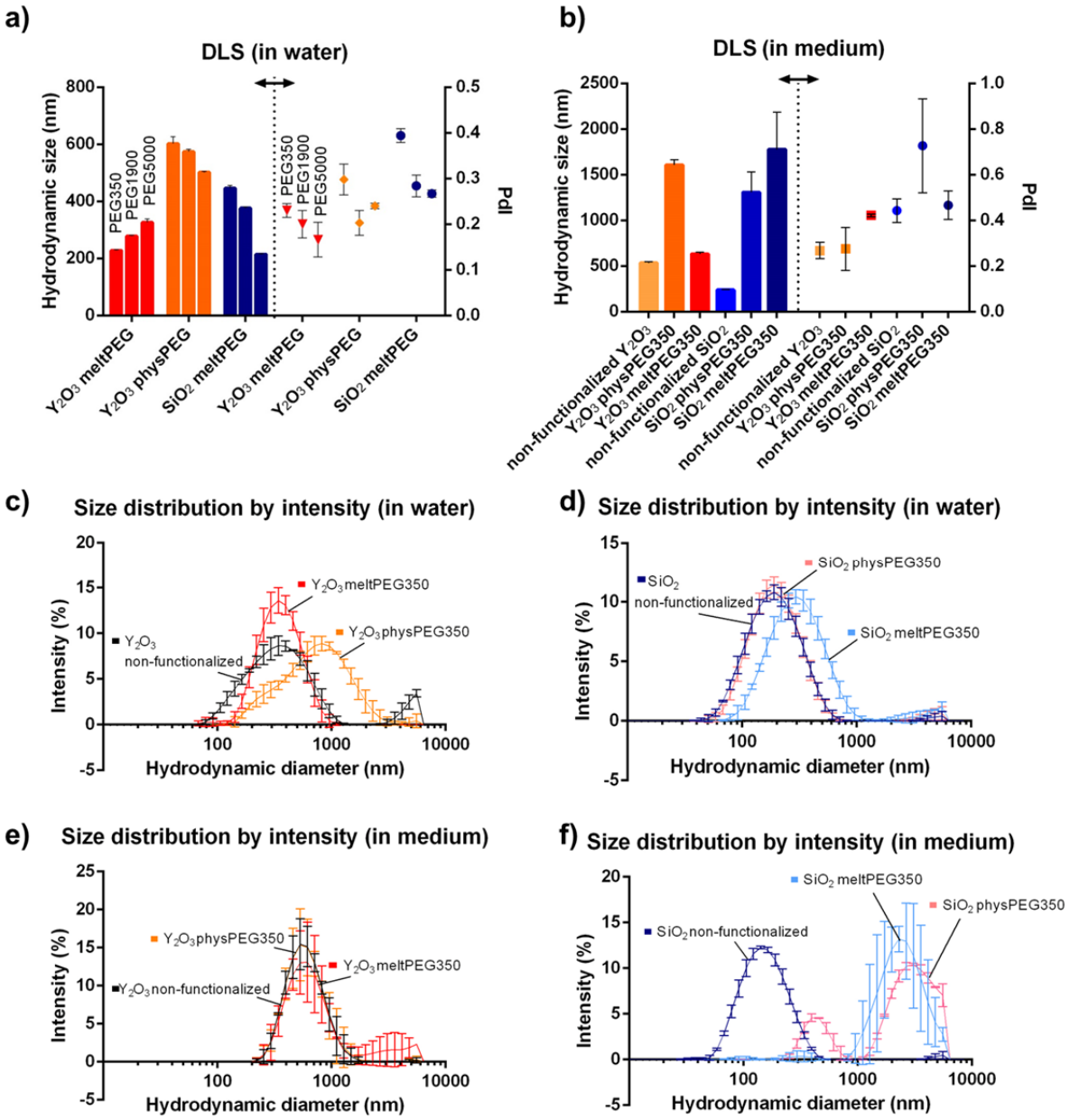

***Figure S3**: Hydrodynamic sizes and polydispersity indices of Y_2O_3:Tb^{3+} and SiO_2 nanoparticles functionalized with different PEG lengths (a). Hydrodynamic sizes in serum-containing cell culture medium (RPMI with 10% serum) for samples with highest grafting densities and their analogues (b). Hydrodynamic size distribution by intensity for Y_2O_3:Tb^{3+} and SiO_2 nanoparticles in water (c, d) and in serum-containing cell culture medium (e, f) measured by DLS.*

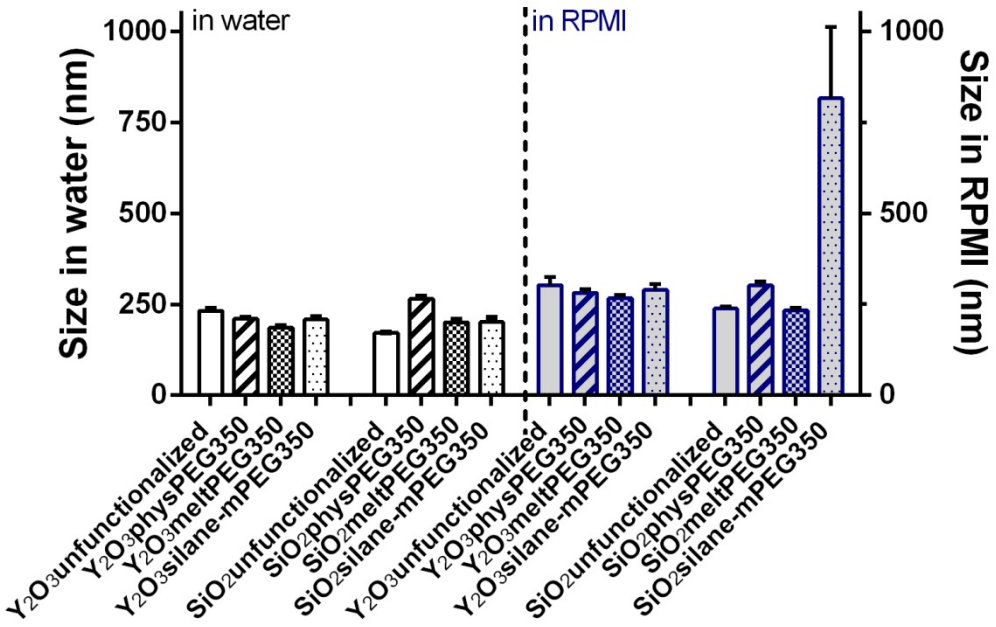

***Figure S4**: Hydrodynamic sizes measured immediately after preparation of the dispersions.*

Calculation of R_F/D values

The average distance *D* between neighboring PEG chains on particle surface determines the structural conformation of the surface-attached PEG chains and thus its shielding effectiveness. If *D* is greater than the Flory radius R_F, that, is, if $R_F/D \leq 1$, neighboring PEG chains will not overlap and are said to be in a "mushroom" conformational regime. However, as the surface PEG density increases such that adjacent PEG chains overlap, that is, if $R_F/D > 1$, PEG chains are forced to stretch away from the particle surface forming a "brush" layer. It is generally believed that surface PEG densities in the mushroom-to-brush transition state are required to offer optimal performance.[8]

The Flory radius R_F of the polymer random coil in a good solvent is expressed as:

$$R_F \sim aN^{0.6}$$

where *N* is the degree of polymerization (the ratio between the polymer's molecular weight and the monomer's molecular weight (ethylene glycol)) and *a* is the effective monomer length (for PEG, $a = 0.35$ nm).[9]

The distance between grafting sites *D* is defined as:

$$D = \left(\frac{4}{\pi\sigma}\right)^{1/2}$$

where σ is the grafting density. This equation assumes that each brush chain occupies a cylindrical volume with its base coincident with the grafting surface.[10]

The grafting densities (chains per nm^2) were calculated based on CHN elemental analysis results and BET surface measurements.

The results obtained for Y_2O_3:Tb^{3+} suggest that while PEG physisorption leads only to a "mushroom" state, meltPEGylation can give access to a "brush" layer. Densities are likely to vary between different particles due to different compositions and availabilities of surface hydroxyl groups.

Table S1.

R_F/D values for yttria nanoparticles.

PEG MW (Da)	*N*	R_F (nm)	*D* (nm)		R_F/D	
			Physisorbed	Melt	Physisorbed	Melt
350	5.6	0.99	1.3	1.0	0.8	1.0
1900	32	2.8	3.0	2.7	0.9	1.1
5000	81	4.9	5.6	4.6	0.9	1.1

R_F/D values for silica nanoparticles.

PEG MW (Da)	*N*	R_F (nm)	*D* (nm)		R_F/D	
			Physisorbed	Melt	Physisorbed	Melt
350	5.6	0.99	8.0	1.3	0.1	0.8
1900	32	2.8	9.9	4.3	0.3	0.7
5000	81	4.9	11.3	5.6	0.4	0.9

References (ESI)

1. Mädler, L.; Stark, W. J.; Pratsinis, S. E. *J Mater Res* **2002,** 17, (6), 1356-1362.
2. Lucky, S. S.; Muhammad Idris, N.; Li, Z.; Huang, K.; Soo, K. C.; Zhang, Y. *ACS Nano* **2015,** 9, (1), 191-205.
3. Spyrogianni, A.; Herrmann, I. K.; Keevend, K.; Pratsinis, S. E.; Wegner, K. *Journal of Colloid and Interface Science* **2017,** 507, 95-106.
4. Sotiriou, G. A.; Schneider, M.; Pratsinis, S. E. *The Journal of Physical Chemistry C* **2011,** 115, (4), 1084-1089.
5. Traina, C. A.; Schwartz, J. *Langmuir* **2007,** 23, (18), 9158-9161.
6. Spyrogianni, A.; Herrmann, I. K.; Lucas, M. S.; Leroux, J.-C.; Sotiriou, G. A. *Nanomedicine* **2016,** 11, (19), 2483-2496.
7. Darmakkolla, S. R.; Tran, H.; Gupta, A.; Rananavare, S. B. *RSC Advances* **2016,** 6, (95), 93219-93230.
8. Suk, J. S.; Xu, Q.; Kim, N.; Hanes, J.; Ensign, L. M. *Advanced Drug Delivery Reviews* **2016,** 99, 28-51.
9. Hansen, P. L.; Cohen, J. A.; Podgornik, R.; Parsegian, V. A. *Biophysical Journal* 84, (1), 350-355.
10. Samadi, A.; Husson, S. M.; Liu, Y.; Luzinov, I.; Michael Kilbey, S. *Macromolecular Rapid Communications* **2005,** 26, (23), 1829-1834.